Original Article

SHM Structural Health Monitoring

Structural Health Monitoring
2016, Vol. 15(3) 247–265

DOI: 10.1177/1475921716636334
shm.sagepub.com
SAGE

An in situ ensemble impact monitoring and identification technique for fiber composite structures under multiple disturbances

Liang Si[1,2] and Horst Baier[1]

Abstract

An investigation is conducted to develop a real-time automatic structural health monitoring technique for the identification and prediction of the locations and force magnitudes induced by foreign objects impacting on composite structures. Accordingly, an in situ ensemble impact monitoring and identification technique is proposed and designed with the usage of distributed sensor networks. Then, the entire impact monitoring and identification mainly consists of four sequential procedures, which are the sensor signal preprocessing, the forward model generator, the impact positioning, and the inverse model operator. In order to achieve good engineering applicability, several uncertainty factors were considered for the composite structures, which are diverse structure configurations, various carbon fiber prepreg layups in the carbon fiber–reinforced polymer specimen panels, and impact conditions. In addition, random interfering noises resulting from structural vibrations were also taken into account as the essential disturbances. Under the different technical conditions and disturbances arising from practical structure vibration environments, the accuracy of the predictions of impact forces and locations using the ensemble impact monitoring and identification technique is validated through a series of impact tests. The errors between estimated and actually measured quantities all fall well within the satisfactory limited range. It is concluded that the ensemble impact monitoring and identification technique is qualified to reconstruct the input forces in sufficient precision due to unforeseen impact events under changeable conditions; it is also able to effectively estimate unknown impact locations in complex adverse environments.

Keywords

Structural health monitoring, fast empirical mode decomposition, hybrid thresholding filtering, fast genetic algorithm estimation, inverse problem, impact identification, composite structures, random vibration noises

Introduction

Modern structures, especially in aerospace application, make increasing use of fiber-reinforced plastic composites, taking advantage of their excellent material properties, such as strength-to-weight ratios, stiffness-to-weight ratios, and corrosion resistance. Fiber composites have a number of advantages over metallic materials, as their material properties can be designed by varying the fiber layup. However, one of the deficiencies of such materials is a high susceptibility to low velocity impact damage. Because they are brittle and capable of withstanding a strain of less than 2% before breaking, a small nick caused by such breakage can reduce the ultimate tensile strength by almost 50%;[1] even this damage in the struck region will be exacerbated owing to the non-visible or limited visual signature on the structural surface. In view of this urgency, the conventional non-destructive inspection (NDI)/non-destructive evaluation (NDE) solution is much difficult to satisfy the demand of the modern design of smart aerospace structures, since the major limitation of this conventional approach cannot provide a continuous assessment of the structural material

[1]Institute of Lightweight Structures, Faculty of Mechanical Engineering, Technische Universität München, Garching, Germany
[2]School of Mechanics and Civil Engineering, China University of Mining and Technology, Beijing, Beijing 100083, P. R. China

Corresponding author:
Liang Si, Institute of Lightweight Structures, Faculty of Mechanical Engineering, Technische Universität München, Boltzmannstr. 15, Garching 85748, Germany.
Email: l.si@tum.de

state.[2] This situation can be significantly improved through the implementation of a structural health monitoring (SHM) system on impact monitoring.[3]

However, over the last 20 years, there has been an extensive amount of research associated with the development of SHM methods including the impact identification aspect for composite and metallic structures. But many researchers did not develop a complete technique or system for locating and reconstructing unknown impacts on a structure. For instance, some investigations[4–6] use appropriate distance angles, arrival times, and optimization techniques such as dispersion compensation, probabilistic approach, and distributed coordination only to locate impacts; some researchers apply various supervised machine learning methods and mapping techniques, which include artificial neural networks[7,8] and ordinary genetic algorithms,[9] and they are capable of modeling complex relations between input and output data; in addition, one class of time-reversal focusing techniques has been applied to locate impact coordinates on isotropic[10,11] and anisotropic[12,13] structures, but most research still adopted the experimental transfer function measuring method. Likewise, they all have only taken into account their tested structure systems under "Perfectly Impracticable Environment Conditions" without any disturbance factors, such as, changeable vibration disturbances from existing engineering environments. Hereupon, in order to realize the engineering applicability for in-service aerospace vehicles, a completely systematic technique needs to be developed for impact positioning and identification (IPI) under complex structure conditions and unpredictable environmental disturbances. The realization of this technique would be very significant for solving practical aerospace engineering problems.

For most impact detection solutions developed, they are very difficult in aerospace vehicles to monitor and identify in real-time unforeseen transient impact events online on board. Accordingly, a novel efficient technique, that is the ensemble impact monitoring and identification (EIMI) technique, is proposed and developed to automatically monitor and real-time report visually the events' occurrences, the occurred locations, and force magnitudes resulting from the impacts under diverse adverse conditions, and it would be very meaningful and helpful at safeguarding the safety and reliability of large-scale aerospace structures. To validate the engineering practicability of the EIMI technique, changeable environmental disturbances and different structure configurations and conditions were designed and applied in this study. In the whole impact monitoring and identification procedure, the functional module of sensor signal preprocessing (SSP) can effectively eliminate complex disturbances from random vibrations using a new filter developed and continuously provide stationary output response signals for the next sequential processing. Next, the functional module of forward model generator can establish more accurate forward models through the fast genetic algorithm estimation (FGAE) for identifying unknown impact events on structures. A forward model is constructed in terms of impulse response functions (IRFs) on the basis of the relations between inputs and outputs, and it can be applicable to various structure configurations and can handle various types of impact objects. Since the forward model provides simple model formulations, the inverse model operator can found rapid calculation models to reconstruct impact forces. Nevertheless, to achieve precise impact positioning, the functional module implements the two-step localization approach, where an initial location can be estimated using the smoothed energy distribution method developed; afterward, an accurate location can be updated further using the time of flight (TOF)-based quadrilateral positioning method proposed, based on the initial estimation region. To interpret the entire IPI procedure, a series of impact tests were performed under different conditions and unpredictable disturbances. The IPI operation becomes more pragmatic, functional, and fast than the conventional model-based identification techniques[14–20] because most of the model-based identification techniques have only established the analytical models for flat and constant property panels. Although Seydel and Chang[14,15] represented a stiffened panel as an equivalent flat plate with varying properties, it is still not easy for complicated structures to obtain a mathematical model, such as analytical model-based approaches or finite element (FE) model, for locating and identifying an unknown impact acting on stiffened composite structures. Even if the model can simulate the structural response well, it is difficult to found a simple inverse formulation to reconstruct impact force from sensor measurement. To sum up, from all the evaluated results, the EIMI technique is competent to online IPI in complex environments and conditions.

Method of approach

This EIMI approach developed is an advanced technique based on global sensor measurements as illustrated in Figure 1, which is adaptable to diverse structure configurations and various types of impact objects. From Figure 1, when an unforeseen impact event acted on a structure, a series of the structural response outputs due to the impact were recorded by the distributed sensor network laid out in the structure. Owing to the effect of vibration disturbances, the original response output signals collected always involved useless random interfering noises, thus they had to be filtered and the effective response outputs are essential

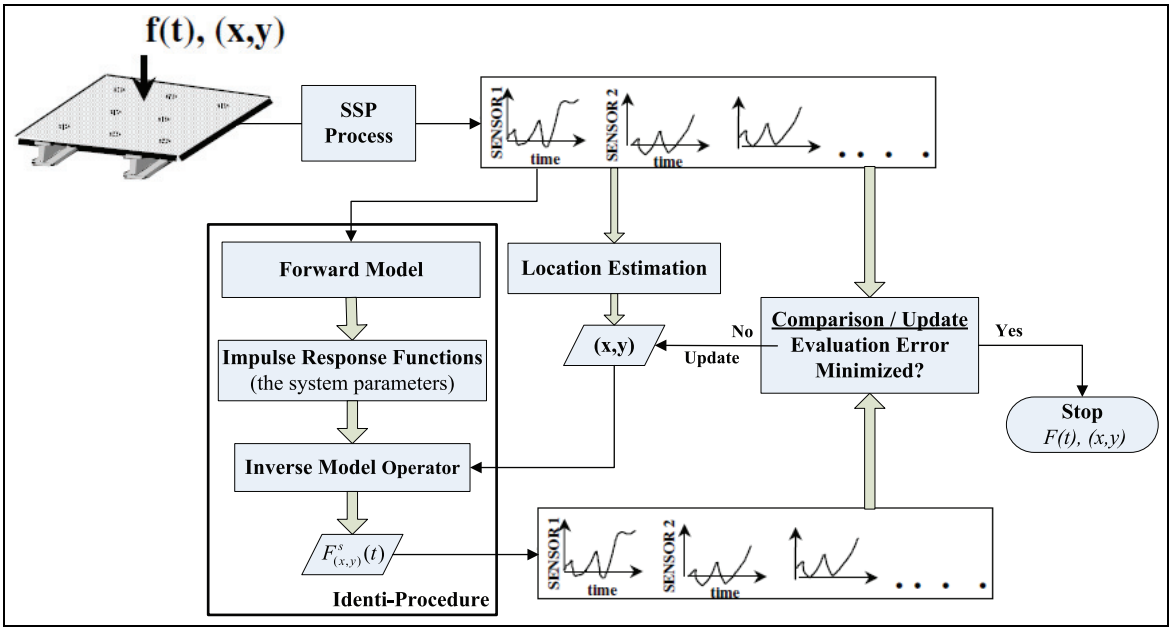

Figure 1. Overview of the systematic frame of the EIMI technique.

to extract through the functional module of SSP. Subsequently, the effective response outputs obtained from the developed filter were used to estimate initially the impact location information, and further the force identification (reconstruction) process could be implemented based on the initial location information. Finally, making use of the propagation property of the stress wave resulting from the impact and the information of the TOF captured from sensor response signals, the location coordinates of the unknown impact would be calculated and updated with the initial location estimation. However, whether the conventional mechanical modeling approaches - model based identification techniques or neural networks based identification techniques, they implement the localizations and force reconstructions due to impacts both based on local sensor measurements, and both have their own irreparable flaws, just as, the conventional model-based identification techniques cannot overcome complex disturbance environments, typically random vibration. As well, they are usually time or labor consuming and are thus intractable and even impossible for complex structures; a great disadvantage of the neural networks–based identification techniques is not applicable for real engineering situations where the types of impactors are not restricted, and also are much difficult to achieve real-time or online diagnosis and evaluation, but only post-processing and estimation. In view of the above background, the methodology of the EIMI technique is proposed and described in the following subsections to indicate its advantages under the complicated conditions, which was mentioned previously. However, this research addresses the impact monitoring and identification problem based on the following conditions:

1. Impacts are constrained to the condition of low velocity;
2. Impact durations are short enough ("millisecond") so that damping does not need to be considered;
3. Impacts do not cause any damage in the tested composite structures. Actually, this EIMI technique proposed is a prognosis technique which predicts impact information under non-damage conditions in a composite structure. However, a reliable safety threshold for the force magnitude or the magnitude of impact energy can be set as the threshold of possible damage, in order to become possibility to perform further damage detection.

SSP

In order to de-noise from original sensor signals, a mode decomposition–based filtering method—fast empirical mode decomposition[21] (EMD)-based hybrid thresholding filter (HTF)[22,23] is adopted to eliminate the disturbances (e.g. random vibration noises) and transfer smoothly the nonlinear effects from non-stationary output signals due to the vibration to the linear dependence; that is, discovering and extracting the effective linear relation between the input and the

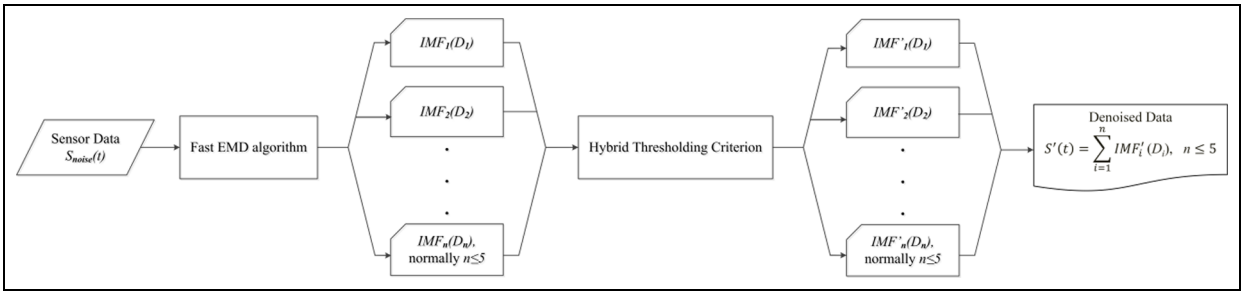

Figure 2. Flowchart of the fast EMD-based hybrid thresholding filtering process.

output from the structural response subject to sudden impact, which is hidden in the nonlinear condition.

The SSP procedure based on the fast EMD-HTF (as shown in Figure 2) is as follows:

1. Sensor temporal signals $S_{noise}(t)$ with random noises are decomposed by fast EMD, as illustrated in Figure 3;
2. From the scales with the valuable information, the first five scales (such as 1st, 2nd, 3rd, 4th, and 5th scales) with the highest energies are extracted normally and then an appropriate threshold is chosen at every scale to remove the interfering noise components. Hence, the hybrid threshold function is defined as

$$IMF'(D_i) = \begin{cases} 0, & \text{if } |IMF(D_i)| < C_1 \\ sign(IMF(D_i)) \cdot \left[\lambda_1 - \sqrt{\left(\lambda_1^2 - C_1^2\right) + (2C_1 + |IMF(D_i)|)|IMF(D_i)|}\right], & \text{if } C_1 \leqslant |IMF(D_i)| < C_2 \\ sign(IMF(D_i)) \cdot \left[\lambda_1 + \sqrt{-C_2(2\lambda_2 + C_2) + 2(\lambda_2 + C_2)|IMF(D_i)| - |IMF(D_i)|^2}\right], & \text{if } C_2 \leqslant |IMF(D_i)| < C_3 \\ IMF(D_i), & \text{if } |IMF(D_i)| \geq C_3 \end{cases} \quad (1)$$

where $IMF'(D_i)$ are the effective components of response signals obtained from the filtering process $i = 1, 2, \ldots, C_2$ is the threshold which will be determined by a kurtosis-based approach individually for every scale and is given by $C_2 = \max(|Z|)/(Kurt(Z)/3)$, where Z is the intrinsic mode function (IMF) coefficient of a scale, $Kurt(Z)$ is kurtosis of the decomposed components. Nevertheless, C_1, C_3, λ_1 and λ_2 will be specified according to the C_2 value in each scale. They are expressed as follows

$$C_1 = \frac{C_2}{p_s} \quad (2a)$$

$$C_3 = \left(1 + \frac{1}{\sqrt{2}p_s}\right) \cdot C_2 \quad (2b)$$

$$\lambda_1 = \left(1 - \frac{1}{p_s}\right) \cdot C_2 \quad (2c)$$

$$\lambda_2 = \frac{1 + \sqrt{2}}{p_s} C_2 \quad (2d)$$

where a specific parameter p_s is defined as $p_s = 1 + \max(Kurt(Z) - 3, 0)$, since a higher kurtosis indicates more significant components existed. In order to make the connection curves tangential at the threshold value, there are two arcs that need to be obtained through calculating the two radii λ_1 and λ_2. This ensures a continuous smooth transition.

The IMF coefficients mainly from the first 5 scales are combined and reconstructed. Finally, the filtered signal can be obtained from the reconstruction process, which is illustrated in Figure 4.

Forward model generator

In the procedure of establishing an accurate forward model, there accomplishes mainly three functions, as follows:

1. Determination of the forward system model structure;
2. Selection of the optimized model order;
3. Minimization of prediction errors and generation of the optimal system parameters (a_i, b_j).

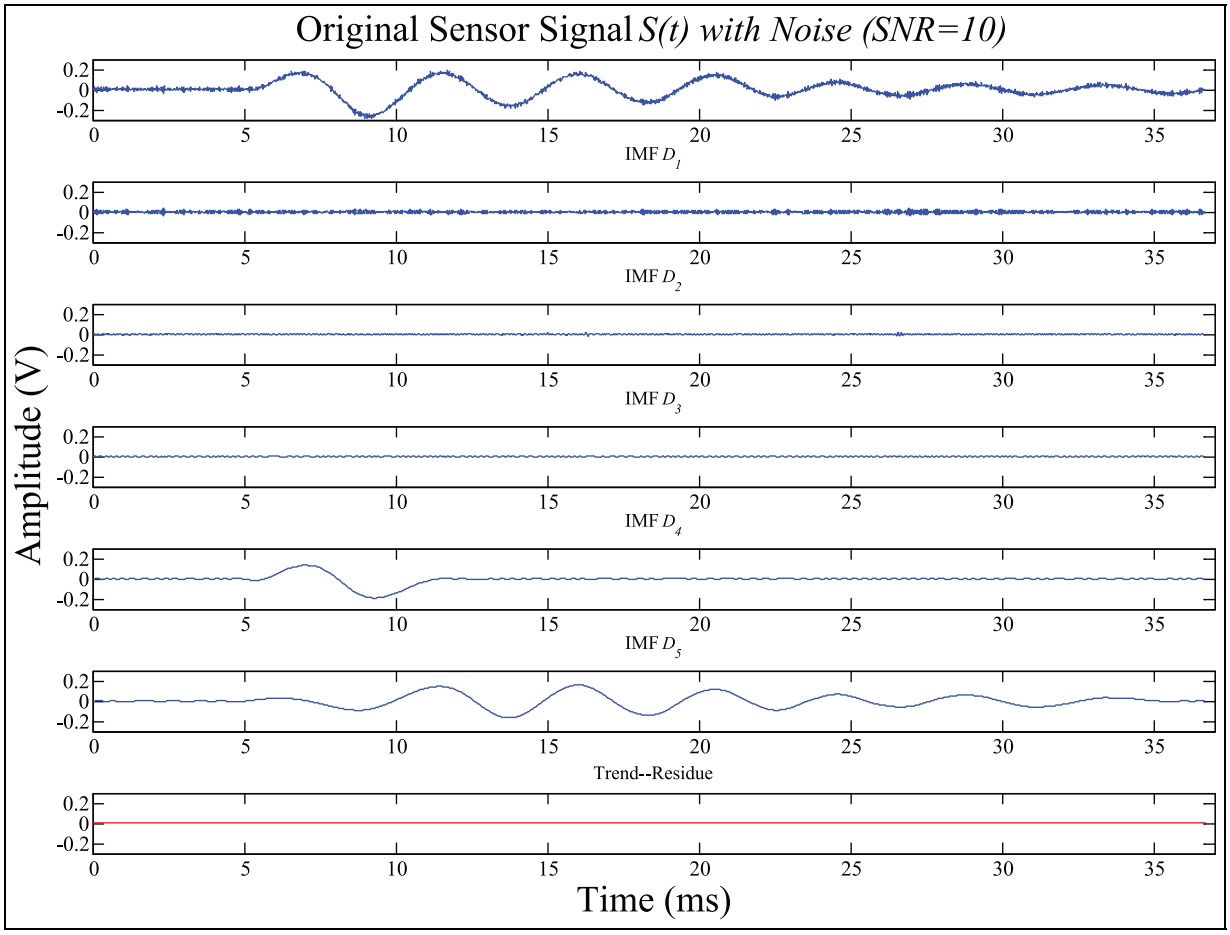

Figure 3. An original output response signal decomposed by the fast EMD.

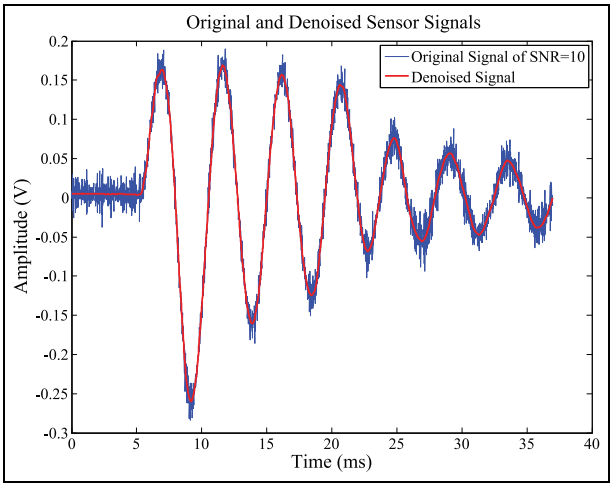

Figure 4. A significant response output de-noised from the original sensor signal.

Determination of system model structure. Considering a structure system model can be applicable to any complex structure, the structure system model of multi-degree of freedom (MOF) by a discrete-time state-space expression[24] is determined and used

$$\dot{x}(k) = Ax(k) + Bu(k) \tag{3a}$$

$$s(k) = Cx(k) + Du(k) \tag{3b}$$

where $u(k)$ is called the input (force) signal, $x(k)$ is called the state vector, $s(k)$ is called the output response signal, and $\dot{x}(k)$ is defined as $\dot{x}(k) = dx(k)/dk$. A is called a structural system matrix, B is called an input matrix, C is called an output matrix, and D is called a feedforward matrix. However, the impulse response (IR) expression given by equation (4) can be derived from the MOF structural system model given by equations (3a) and (3b)

$$s(k) = \sum_{i=0}^{k} g(i)u(k-i) \qquad k = 1, 2, \ldots \tag{4}$$

where IR function

$$g(0) = D \qquad g(i) = CA^{i-1}B$$
$$\text{the matrix component number} \qquad i = 1, 2, \ldots \tag{5}$$

Therefore, now it is much important to find out the relationship between the input force signals $u(k)$ and the output sensor signals $s(k)$. In other words, the objective of forward system modeling is to describe $s(k)$ as a function of previous outputs and inputs, and together with noises $e(k)$. Thus, a set of models[25] is postulated, within which the best description of the true structure system will be searched for

$$s(k) = [1 - A(q)]s(k) + B(q)u(k) + e(k) \tag{6}$$

where the symbol q is the time shift operator defined by $s(k-n) = q^{-n}s(k)$. $e(k)$ is a sequence of uncorrelated random noises. Since $e(k)$ has been de-noised through SSP procedure as described in the section "SSP," the IR representation related between input and output can be thus modeled through the following equation (7)

$$\hat{s}(k|\theta) = \sum_{i=1}^{n} a_i s(k-i) + \sum_{j=1}^{m} b_j u(k-j) \tag{7}$$

where the parameterized model vector $\theta = [a_1 \ldots a_n \quad b_1 \ldots b_m]^T$.

Equation (7) is called the predictor of output sequence $s(k)$, that is, known as the forward system model.

Prediction error minimization–assisted model order selection. Here, a criterion of model order selection need to be defined, which is to minimize the prediction error between the modeled output and the real response output separately from the simulated system model and the real structure system. Accordingly, an optimal output model with the best model order will be established finally. Therefore, to select the appropriate model order, the following selection criterion is used:

1. Start with a smallest model possible (normally the model orders $2 \leqslant n \leqslant 8$);
2. Increase model order until the recursive coefficient Ω^2 is high enough and close to 1

$$\tilde{\varepsilon}(k) = \varepsilon\left(k, \tilde{\theta}\right) = \varphi^T(k)\tilde{\theta} - s(k) \tag{8}$$

$$\Omega^2 = 1 - \frac{\sum_{k=1}^{n} \tilde{\varepsilon}^2(k)}{\sum_{k=1}^{n} s^2(k)} \tag{9}$$

where $\tilde{\varepsilon}(k)$ is the prediction error; $\varphi(k)$ is the regression vector as follows

$$\varphi(k) = [\,-s(k-1) \quad \ldots \quad -s(k-n) \quad u(k-1) \quad \ldots \quad u(k-m)\,]^T$$

$\varphi^T(k)\tilde{\theta}$ is an predicted output model simulated from the proposed FGAE, of which the details will be described in section "FGAE-assisted IR functions generator."

3. If Ω^2 is high enough and increasing model order does not help increasing the value of Ω^2, select the model with the smallest order.

FGAE-assisted IR functions generator. To minimize the prediction errors between the real outputs and the modeled outputs for obtaining the optimized forward system model, and to further obtain the required IR function matrix from the system parameters (a_i, b_j) calculated, a fast GA[26] estimation method[27] is defined and applied into the optimization procedure of the values of (a_i, b_j) solved from the forward system modeling by training rapidly the input–output data collected.

In the fast genetic algorithm–based error estimation procedure, there are normally the five genetic operations need to execute, which are reproduction, crossover, mutation, new blood, and elite. Then, a multi-entropy $H(a_n, b_m)$ has to be defined shown in equation (10) to minimize the prediction error through the FGAE training method proposed

$$\tilde{\theta}[a_n, b_m]_{opt} = H(a_n, b_m) \tag{10}$$

where $\tilde{\theta}[a_n, b_m]_{opt}$ is an optimized parameter vector, which serves to found the optimal response output model. The entropy $H(a_n, b_m)$ is decomposed into two factors $H(a_n)$ and $H(b_m)$ shown in equations (11) and (12)

$$H(a_n) = -\sum_{i=1}^{n} P(a_n) \log P(a_n) \tag{11}$$

$$H(b_m) = -\sum_{i=1}^{m} P(b_m) \log P(b_m) \tag{12}$$

In contrast to the conventional parameter estimation methods such as the least squares error estimation (LSEE), the FGAE shows its more significant advantages over LSEE. First, the FGAE has a distinct feature of adjustable genetic parameters such as error tolerance, population size, mutation rate, and number of iterations, which are illustrated in a graphical user interface (GUI) (called the fast genetic algorithm identification interface) developed by MATLAB® as shown in Figure 5. Owing to the dominant feature of FGAE, it is more accurate than LSEE for estimating the system

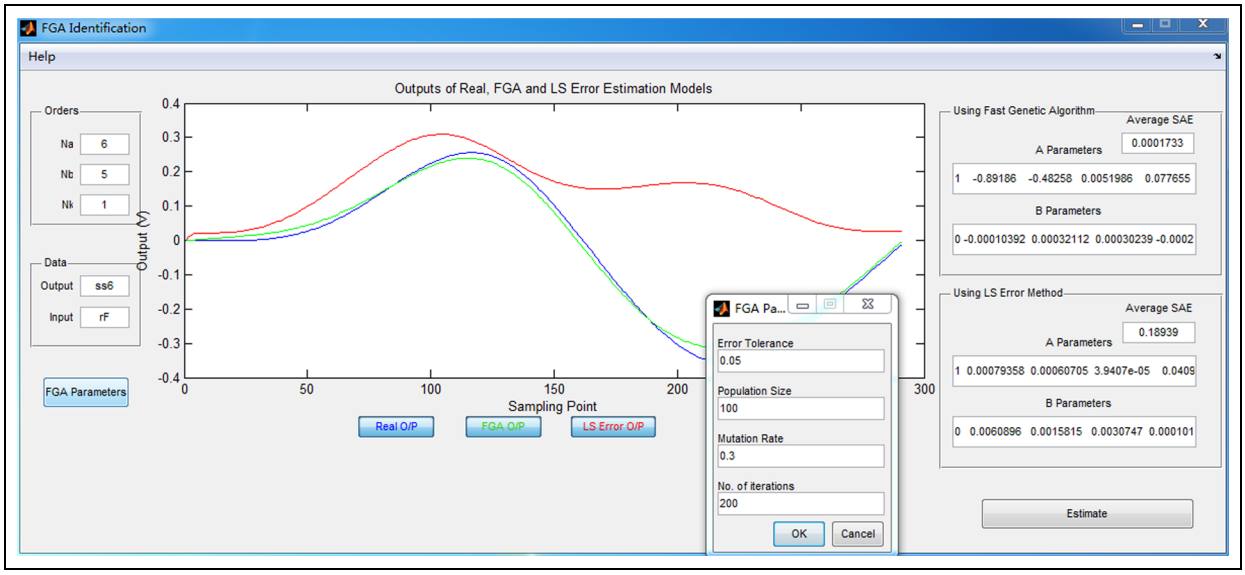

Figure 5. System parameters (a_i, b_j) estimation in the developed FGA identification interface.

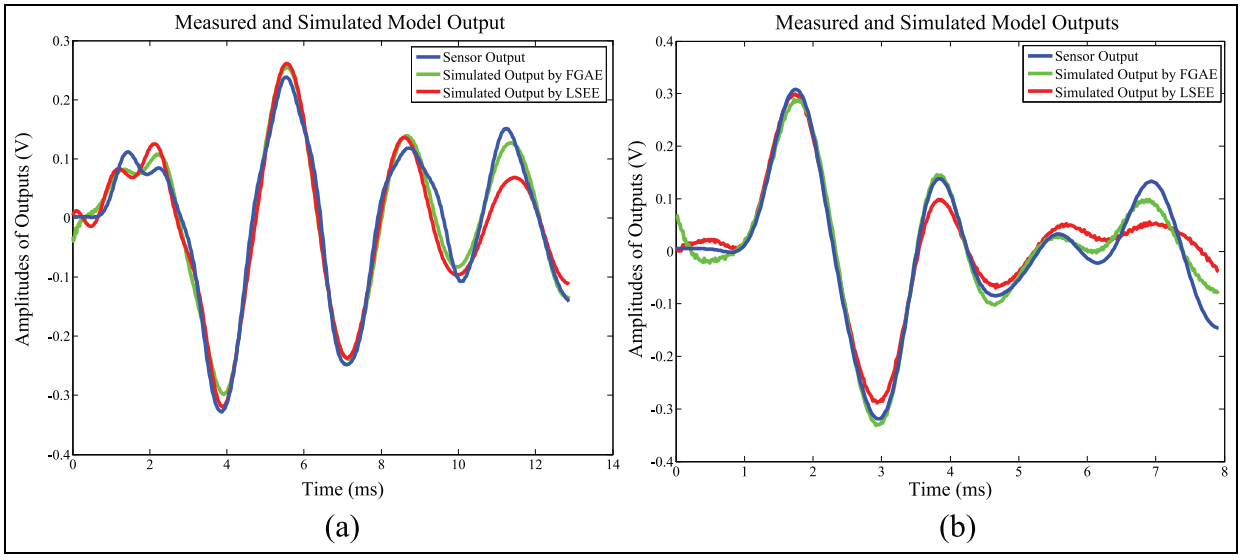

Figure 6. Verifications of forward models: (a) model validation with a plastic impact tip and (b) model validation with a steel impact tip.

parameters (a_i, b_j) because the LSEE only has a non-advantageously uniform feature from the linear parameterization and quadratic criterion to estimate the system parameters. Second, the accuracy of the outputs of the forward model simulated by the FGAE is higher than that of the LSEE, which is presented in Figure 6. Third, in order to ensure the robustness and stability of an estimated system model, a means of zeros and poles is chosen as a way to inspect the state of the system model so that the corresponding inverse model also becomes robust and stable in the impact force identification (reconstruction). When the system parameters estimation procedure picks out the "best" system model within the chosen model structure, the robustness and stability of the system model need to be examined by checking the pole-zero plane of the system model. Through the examination of the pole-zero plane, the system model and its inversion should be both robust and stable so that this "best" system model is "good enough." In other words, all poles and zeros from the model should be inside the unit circle. Hence, as a great many system models built using the FGAE

and LSEE were examined and compared, the models generated using the FGAE were more robust and stable than that of the LSEE.

Finally, the IR function matrix G_{μ}^{s} demanded can be obtained using equation (13)

$$G_{\mu}^{s} = \begin{bmatrix} g(0) & 0 & 0 & \Lambda & 0 \\ g(1) & g(0) & 0 & \Lambda & 0 \\ M & M & O & 0 & M \\ g(n-2) & g(n-3) & O & O & 0 \\ g(n-1) & g(n-2) & \Lambda & g(1) & g(0) \end{bmatrix} \quad (13)$$

However, the IR $s(k)$ of a structure system can be represented in a matrix convolution formulation given by equation (14)

$$S_{(x',y')} = G_{\mu}^{s} U_{(x,y)} \quad (14)$$

where

impulse input $U_{(x,y)} =$

$$[u(0) \quad u(1) \quad u(2) \quad \ldots \quad u(n-1)]^{T} \quad (15a)$$

reason output $S_{(x',y')} =$

$$[s(0) \quad s(1) \quad s(2) \quad \ldots \quad s(n-1)]^{T} \quad (15b)$$

In that way, in order to indicate the accuracy of forward models simulated through the FGAE, the simulation results are compared with the real sensor signals and the modeled outputs using the LSEE, as shown in Figure 6. This figure reveals intuitively that the predicted outputs from the FGAE align well with the real outputs; on the contrary, the predicted outputs using the LSEE are not better than that of the FGAE.

Inverse model operator

In order to reconstruct impact forces, the force signals from impacts can be predicted based on the inverse model operator using the output data of the structure responses. Then, through applying the structure system model (equations (3a) and (3b)) combined with the IR

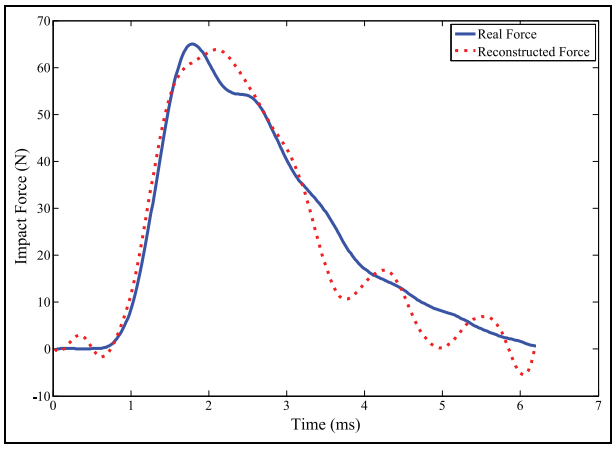

Figure 7. Demonstration of an impact force reconstruction.

expression (equation (4)) described in section "Determination of system model structure," the inverse IR model for force reconstruction is found and the corresponding force signals due to impacts can be also calculated by the defined inverse procedure.

Supposing the reconstruction of the impulse force $\boldsymbol{u}$ at time k is a function of the corresponding response $\boldsymbol{s}$ at times $[k+1 \quad \ldots \quad k+r]$. Thereupon, the IRFs at time sequence $[0 \quad 1 \quad \ldots \quad r-1]$ would be all zero. Accordingly, on the basis of the assumption of zero initial conditions, the inverse IR model is established as follows

$$u(k) = \sum_{i=0}^{k} \hat{g}(i) s(k+r-i) \quad k = 1, 2, \ldots \quad (16)$$

where the inverse IR function matrices are defined by

$$\hat{g}(0) = (CA^{r-1}B)^{T} \hat{g}(i) = \hat{C}\hat{A}^{i-1}\hat{B} \quad i = 1, 2, \ldots \quad (17)$$

Finally, an impact force which is applied at the location (x, y) on a structure can be reconstructed through equation (18) that is the matrix convolution expression of equation (16). And an example of force reconstruction is illustrated in Figure 7

$$U_{(x,y)} = \begin{bmatrix} u(0) \\ u(1) \\ \vdots \\ u(N-r-2) \\ u(N-r-1) \end{bmatrix} = \begin{bmatrix} \hat{g}(0) & 0 & 0 & \cdots & 0 \\ \hat{g}(1) & \hat{g}(0) & 0 & \cdots & 0 \\ \vdots & \vdots & \ddots & 0 & \vdots \\ \hat{g}(N-r-2) & \hat{g}(N-r-3) & \ddots & \ddots & 0 \\ \hat{g}(N-r-1) & \hat{g}(N-r-2) & \cdots & \hat{g}(1) & \hat{g}(0) \end{bmatrix} \begin{bmatrix} s(r) \\ s(r+1) \\ \vdots \\ s(N-2) \\ s(N-1) \end{bmatrix} \quad (18)$$

Estimation of impact locations

To determine multi-impacts locations and decrease the estimation time for impact locations and reconstructions, an initial estimation method is essential to be defined and adopted. Hence, a smooth energy distribution method is proposed to search and identify the sensors closest to the impact points, which is rapid and accurate to locate the impacted regions without the susceptibility from any measurement noise. While, this method allows one or multiple regions of sensor array to be formed and isolated, afterward distribute to update the accuracy locations of impact forces.

Extraction of impact region. By comparing the energies in the chosen time windows of sensor data, the close sensor array are determined and the corresponding energies from the sensor signals can be calculated as

$$E_i = \sum_{k=t_0}^{t_1} s_{exp}^2(k) \tag{19}$$

where E_i is the energy of the each sensor interested, s_{exp} is the experimental signal data recorded from the selected sensor, t_0 is the initial time point, and t_1 is the final time point chosen. As for the selection of the interested time window, it should be determined from a chosen sensor signal so that a sensor array close to each impact detects a great deal of energy but other sensor arrays far away detect a descending amount of energy until the amount of energy detected falls close to zero.

Once impacts occur, the energy of each sensor signal can be calculated in a chosen time window using equation (19). When the energy values are calculated at each sensor position in a structure, a smooth energy distribution with minimum curvature can be found using the Robust Loess Smoothing method,[28] and then the smoothed energy distribution can be expressed in terms of x and y coordinates, as follows

$$E_i = E_i(x_i, y_i) \quad i = 1, 2, \ldots \tag{20}$$

Using the smoothed energy distribution found in equation (20), an impact location can be estimated in terms of the centroid of the corresponding impulse energy. In the x and y coordinates system of a structure, the centroid can be given by

$$x_c = \frac{\sum E_i \cdot x_i}{\sum E_i} \quad y_c = \frac{\sum E_i \cdot y_i}{\sum E_i} \tag{21}$$

where x_c is center of the x axis and y_c is center of the y axis.

In experimental tests implemented, a carbon fiber–reinforced polymer (CFRP) cantilever structure was used to verify that this method provides a reliable and effective way to isolate an impacted region made up of sensor array, regardless of the conditions of vibration noise contamination. The following Figure 8 demonstrates the extraction of the impact region by the smooth energy distribution method proposed.

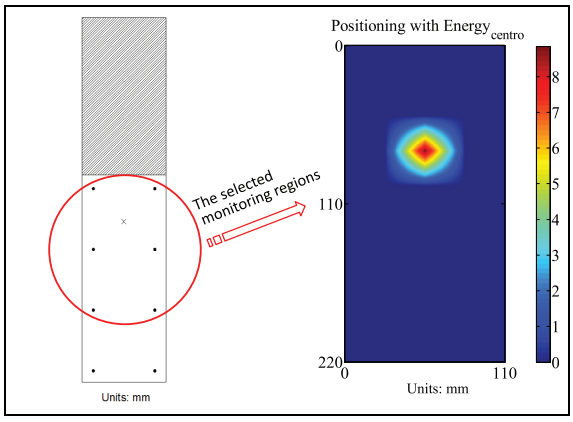

Figure 8. Estimation of the initial location for an unknown impact event.

Locating impact coordinates. To update the precise locations of impact forces on a structure, an effective search parameter index—TOF—is defined and applied, which is an important characteristic parameter that represents the propagation of stress waves in a structure. In order to obtain the parameter of TOF, with the premise of the zero initial condition, the time of arrival needs to be determined by selecting the minimum before the maximum for each sensor response signal.

Within an identified impact zone composed of four neighboring sensors, using the initially assumed wave propagation angles θ_i, the initial distance L_i between an unknown impact position and every sensor S_i can be calculated first in equation (22), and four initially estimated impact positions resulting from L_i are also obtained simultaneously. Then a quadrilateral is composed of those positions. Finally, to obtain the accurate impact coordinates, a procedure to minimize the area of the dashed quadrilateral needs to be executed, as shown in Figure 9. A final estimation of the unknown impact coordinates can be calculated with the principle of the quadrilateral centroid, which is expressed in equations (23) and (24)

$$L_i = C_p(\theta_i) \times \Delta T_i \quad i = 1, 2, 3, 4 \tag{22}$$

where $C_p(\theta_i)$ is the phase velocity of stress waves with the deflection angle of the propagation path from the impact to sensor S_i. Meanwhile, four different angles (namely, θ_1, θ_2, θ_3, and θ_4) for wave propagation

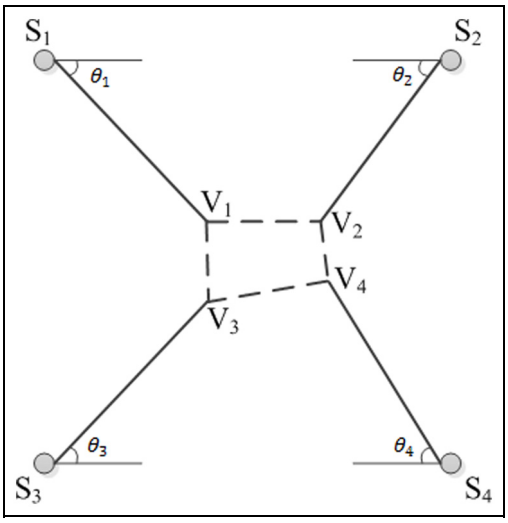

Figure 9. Demonstration of updating impact coordinates with the quadrilateral centroid.

directions are assumed. Additionally, ΔT_i is the TOF for sensor S_i. Thus, an unknown impact location (X_{imp}, Y_{imp}) can be estimated by

$$X_{imp} = \frac{1}{6M}\sum_{i=1}^{4}(x_i + x_{i+1})(x_i y_{i+1} - x_{i+1} y_i) \tag{23}$$

$$Y_{imp} = \frac{1}{6M}\sum_{i=1}^{4}(y_i + y_{i+1})(x_i y_{i+1} - x_{i+1} y_i) \tag{24}$$

where M is the area of the quadrilateral, $M = \frac{1}{2}\sum_{i=1}^{4}(x_i y_{i+1} - x_{i+1} y_i)$. x_i and y_i are the x and y coordinates for the vertices V_i (i = 1, 2, 3, 4), respectively. The entire procedure is presented graphically in Figure 9 and can be implemented for any configuration of a quadrilateral sensor network.

Experimental details and procedure

With the theoretical development and computer implementation of the EIMI technique, it is necessary to set up the experimental tests for some specific practical applications so as to validate the EIMI technique's effectiveness and practicality. Subsequently, the experimental tests were performed on two CFRP panel structures with the different impact conditions and various surrounding noise environments. Among them, specimen 1 is a narrow CFRP plate without any stiffener and specimen 2 is a square CFRP panel with one stiffener.

Experimental specimens

Specimen 1 (as Figure 10(a)) is a CFRP plate with the dimensions of 660 mm × 150 mm × 5 mm, and its layups are adopted as $[0°, 90°]_w/[0°/90°]_{8s}/[0°, 90°]_w$. Meanwhile, the sensor interval is chosen as 110 mm × 110 mm, which is shown in Figure 10(a). And specimen 2 is also a CFRP panel with a T-beam stiffener running the length of the panel. Its layups are adopted as $[0°, \pm 45°, 90°]_{4s}$. The sizes of specimen 2 are 390 mm × 390 mm × 3 mm, and its sensor interval is shown in Figure 10(b).

Two different distributed piezoelectric sensory networks and associated wirings were mounted individually on the backward surfaces of two CFRP panel structures, which are considered from the perspective of practical engineering demands and are also convenient to impacts on the forward surfaces of two CFRP panels by an instrumented hammer and several small balls. In order to ensure good surface conduction at sensor locations, the surfaces of two CFRP panels were sanded and a small amount of conductive epoxy was applied.

Experimental setup

They are first more important basis for impact monitoring and identification to select the appropriate sensor material, to design the rational shape, and to determine the applied sizes. Accordingly, one kind of small circular lead zirconium titanate disc sensor (as Figure 11) was designed and used to measure the non-directional strain property, which was polarized in the z-direction that is the thickness direction. The diameter of every sensor used is 5 mm, and its thickness is 0.25 mm. In addition, the two CFRP panels as specimens were impacted by a hand-held, instrumented hammer manufactured by PCB Piezotronics. Both the force signals from the impact hammer and the sensor output data from the structural responses were recorded using a computer data acquisition (DAQ) system manufactured by Labortechnik Tasler. Also, a function/arbitrary waveform generator and a power amplifier were utilized to actuate a piezo composite stack to act as a vibrator (shaker), thereby a series of repetitive random vibration disturbances were generated from the piezo-vibrator (or called the piezo-shaker) and were propagated in the composite structure. All sensor data were collected at the different sampling rates which are from the sampling rate of 25–50 kHz, and the corresponding amplitudes were controlled in the range of ±15 V.

The two specimens were used to verify the adaptive forward models established, to assess impact locations estimations, and to evaluate the applicability of the EIMI technique due to the diversifications of composite materials, structure configurations, the types of impactors, and the unpredictable environmental disturbances that are typically random vibration noises.

Meanwhile, for specimen 1, it was fixed on one side and the other side was free, which was built as a cantilever structure shown in Figure 12. For specimen 2, it

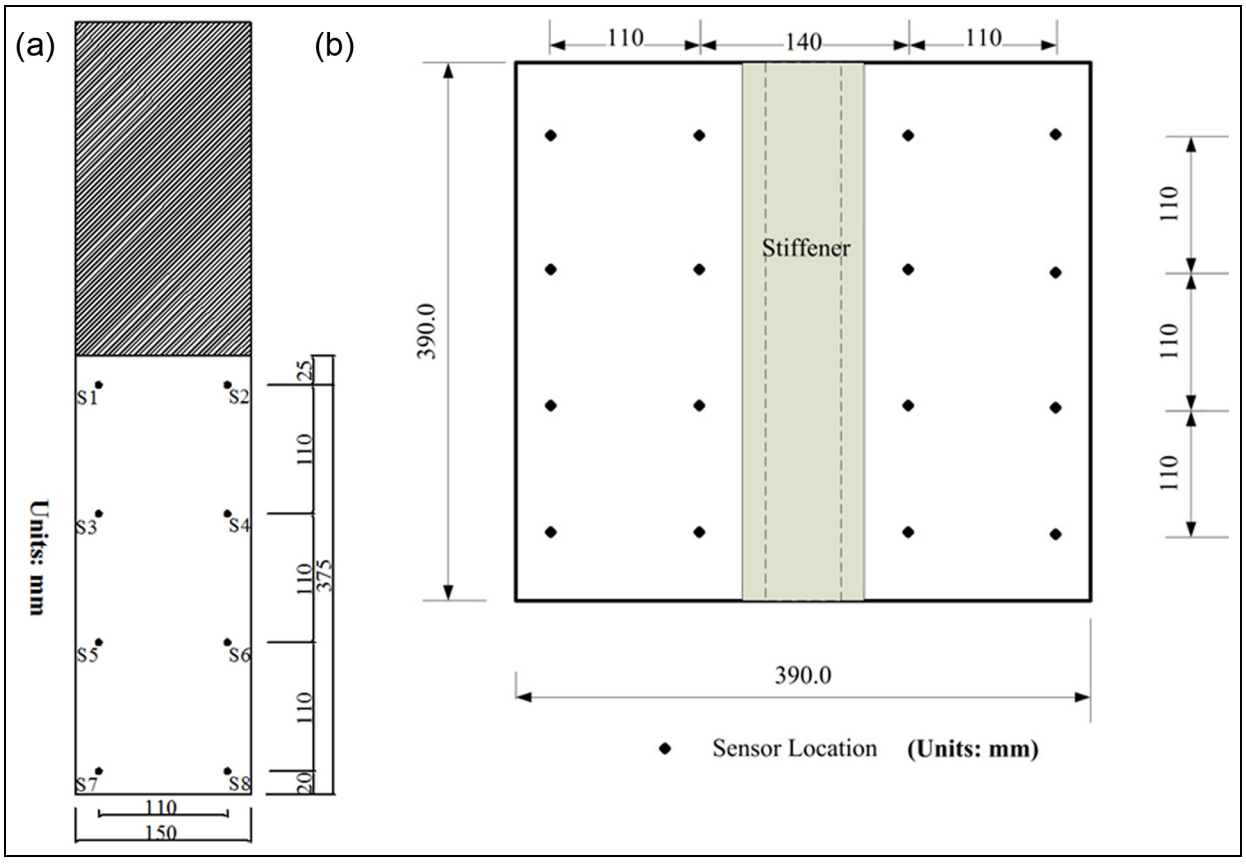

Figure 10. Geometries of the CFRP specimens and their sensor locations: (a) specimen 1 and (b) specimen 2.

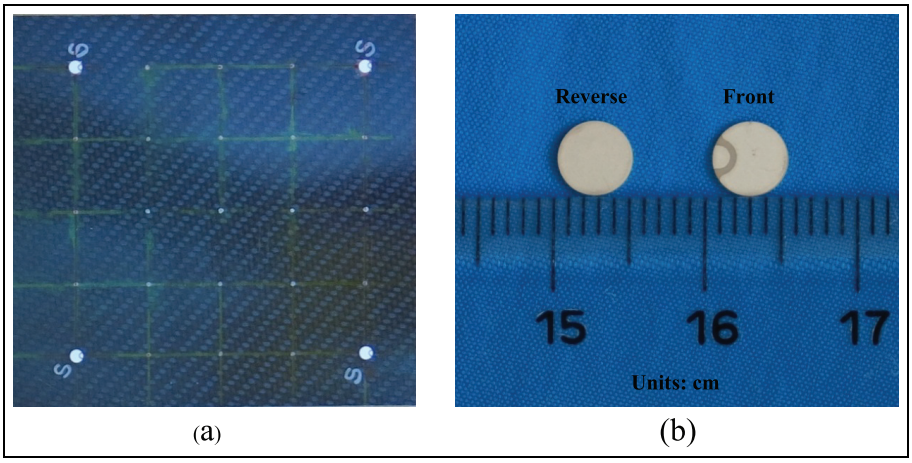

Figure 11. Piezoelectric disc sensors used to measure strain data: (a) sensors mounted on a CFRP structure and (b) sensor prototype.

was supported by four columns at the corresponding four corners.

Impact tests

In order to obtain the various IRFs, the impact experimental tests were performed over the two specimens. For forming the network nodes of the various IRFs, force signals and sensor signals from the structural responses were recorded (1) from 65 points of impact tests on specimen 1 and (2) from 54 points of impact tests on specimen 2. Their schematic demonstrations are shown in Figure 13, where the experimental impact

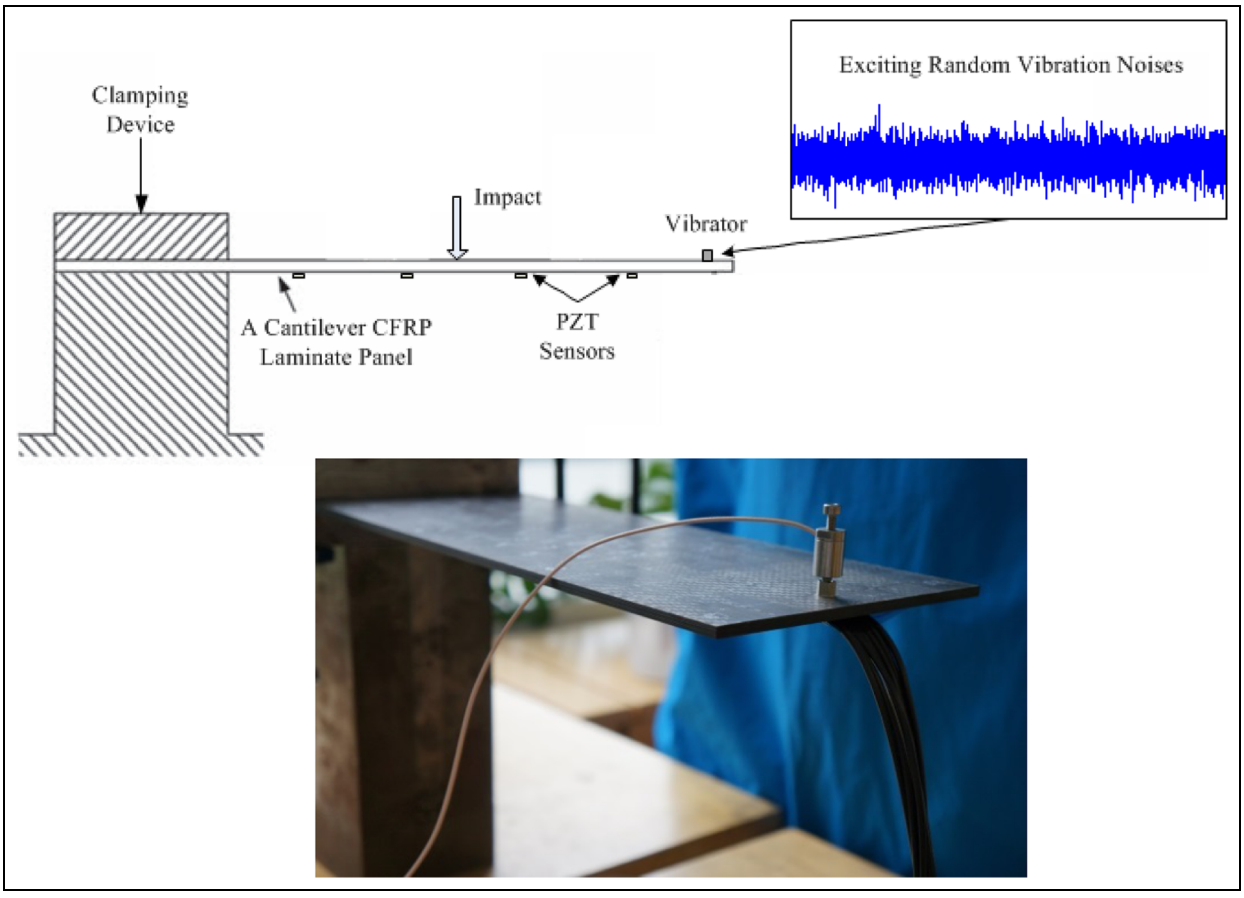

Figure 12. Boundary and environmental conditions for specimen 1.

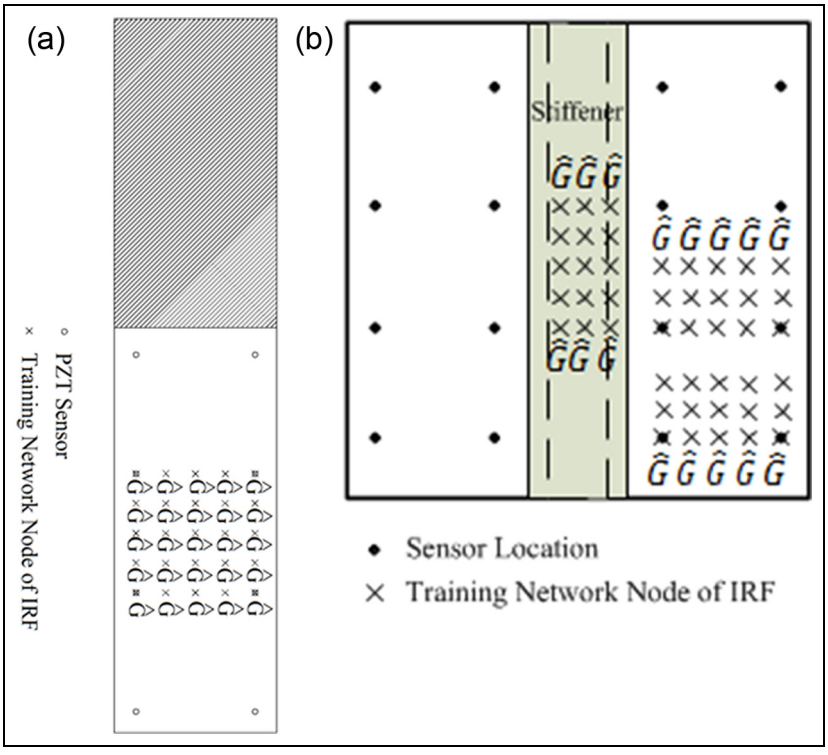

Figure 13. Demonstration for the formation of IRF networks: (a) specimen 1 and (b) specimen 2.

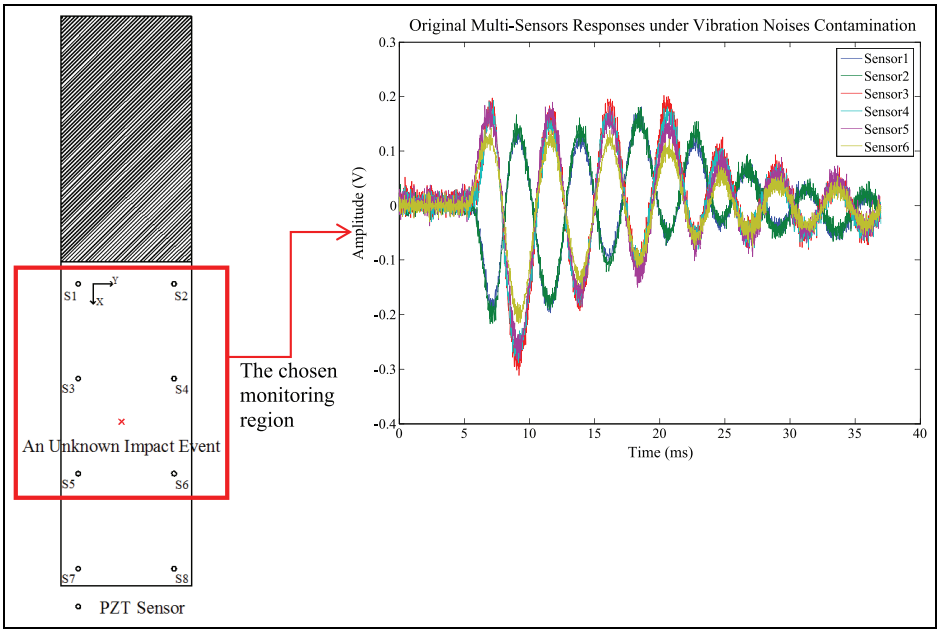

Figure 14. Original multi-sensor response signals under vibration noises contamination.

points were made at evenly spaced locations, and random force magnitude was applied at each location. Once the corresponding networks made up of the IRF nodes are constructed individually for specimen 1 and 2, various impact tests can be made at any arbitrary location in spite of on specimen 1 or 2. Additionally, a series of verifications on impact identifications can be implemented effectively. In impact tests, a set of original multi-sensor response signals due to an impact event were recorded under random vibration environments, as presented in Figure 14.

Results

The estimated and reconstructed results are illustrated to validate the efficacy of the EIMI technique for impact source identification. Then, the issues around the assessments of estimated impact locations, the effects of various anisotropic structure configurations on force reconstructions, and the effects of random vibration noise contaminations on force reconstructions will be discussed in detail as follows.

Impact location estimations and error evaluations

To illustrate the proposed performance of impact positioning and its accuracy under various impact conditions, two sets of representative impact conditions were selected from a series of impact validation tests, where for specimen 1, an unknown impact event acted in the boundary vicinity of the cantilever structure, and the other unknown impact event acted in the middle region of the structure; for specimen 2, an unknown impact event acted in the stiffener region of the stiffened structure, and due to the structural symmetry, the other unknown impact event acted in the right bay of the structure. Hence, the two sets of the estimated results for impact locations on specimens 1 and 2 are shown, respectively, in Figures 15 and 16. Whether specimen 1 or specimen 2, the origins of their x-y coordinate system were both selected at the location point of sensor S1. Nevertheless, as for specimen 1, the x-direction is defined as the length direction of the CFRP plate; as for specimen 2, the y-direction is defined as the direction of the stiffener.

Afterward, in order to assess the estimated impact locations, the location error evaluated is defined in equations (25)–(27), which is expressed as the distance from the calculated impact location to the actual impact location

$$\Delta x = x_{cal} - x_{act} \tag{25}$$

$$\Delta y = y_{cal} - y_{act} \tag{26}$$

$$\zeta_e = \sqrt{\Delta x^2 + \Delta y^2} \tag{27}$$

The average positioning error ratio (APER) e_p still needs to be defined as

$$e_p = \frac{1}{N}\sum_{1}^{N}\frac{\zeta_e}{I_s} \times 100\% \tag{28}$$

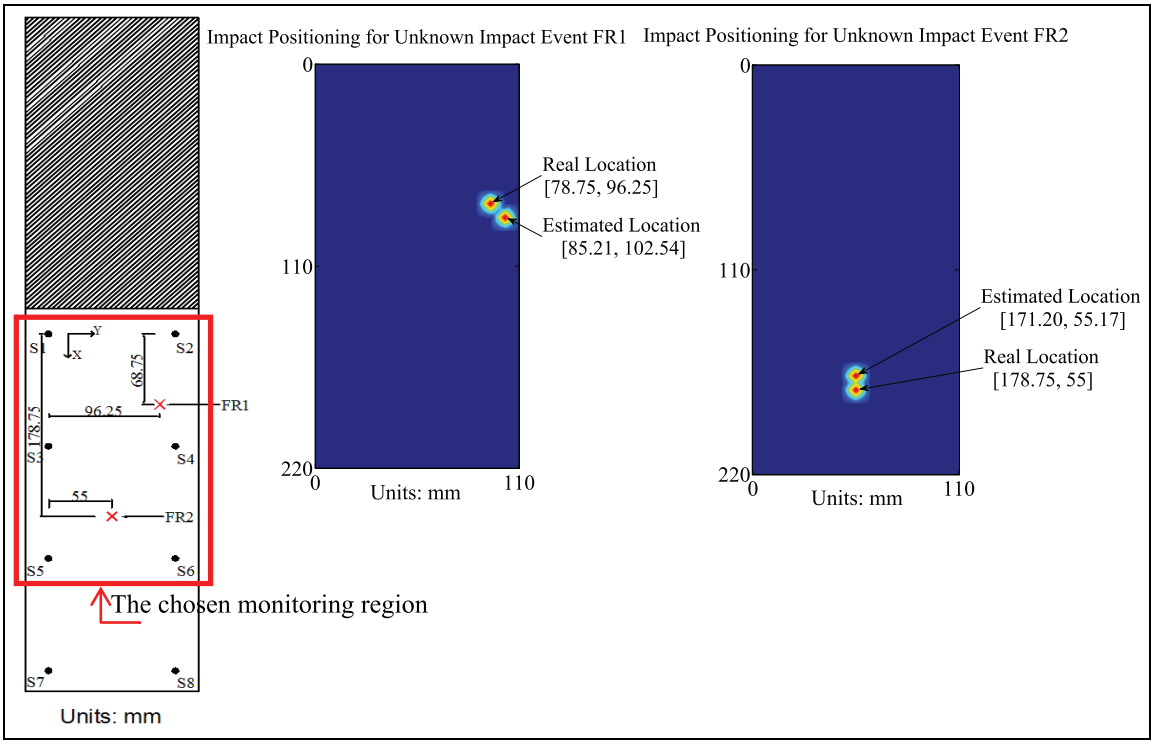

Figure 15. Location estimations of two unknown impact events on the cantilever structure.

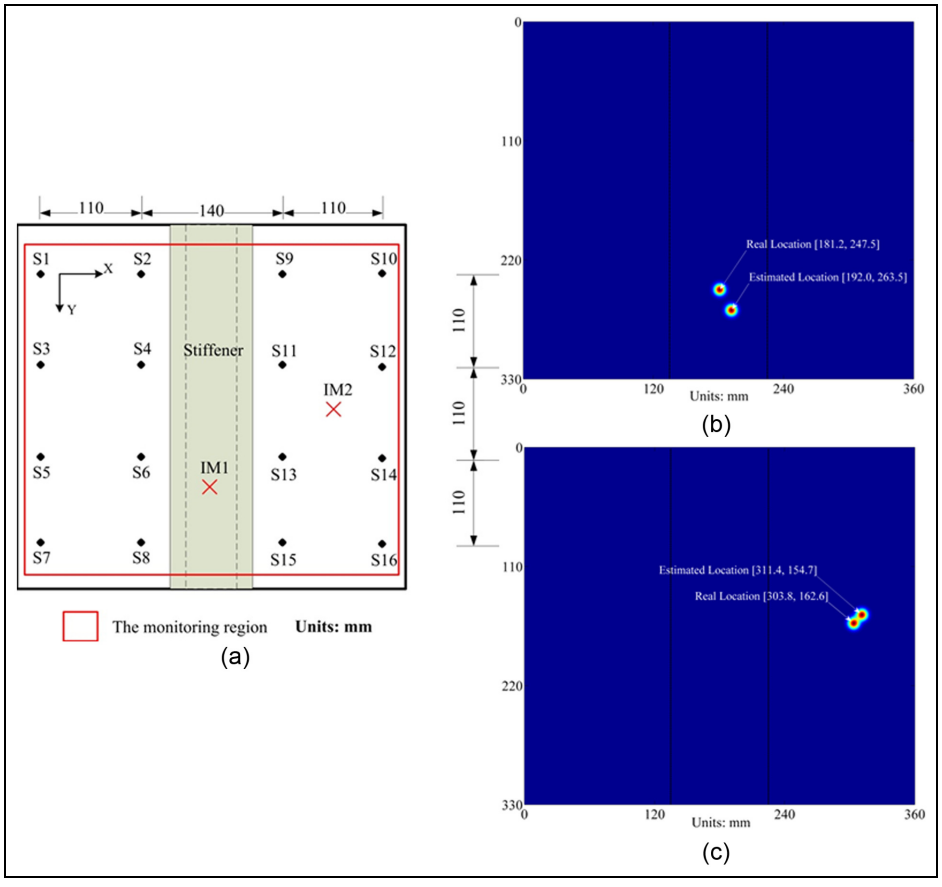

Figure 16. Location estimations of two unknown impact events on the stiffened structure: (a) the test layout, (b) impact on the stiffener, and (c) impact on the right bay.

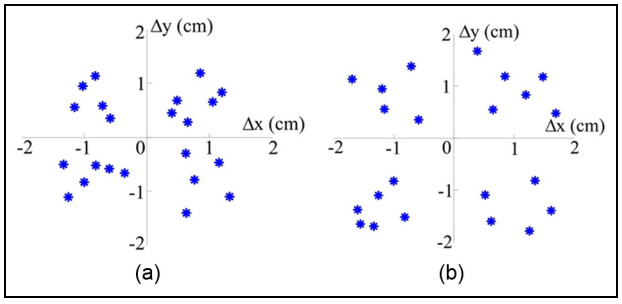

Figure 17. Location estimation errors for unknown impact events on: (a) specimen 1 and (b) specimen 2.

where I_s is referred to the interval between the laid sensors.

Through a series of impact verification tests on specimen 1 and 2, generally the average location errors are mostly in the range of 10.3% and 11.8% of the corresponding sensor interval mounted, respectively, which are shown in Figure 17.

Impact identifications and error evaluations

Typical impact identification tests were performed to validate the force-reconstruction function module for various composite structure configurations. However, various IR function matrix networks for various types of composite structures (as specimen 1 and 2) were obtained firstly from two different approaches, which are that the one utilizes the simulated output data from the built FE models and the other one adopts the output data from a series of corresponding impact training. Hence, using the various IRF matrix networks found, the procedure of force reconstructions is implemented easily for unforeseen impacts on various types of composite structures.

The simulated results of force reconstructions on the different composite structures are shown in Figures 18 and 19. In order to interpret the universal performance of the EIMI technique, some representative impact cases were selected. For specimen 1, the impact location FR1 was selected due to the consideration of boundary performance validation for the EIMI technique, and the impact location FR2 was selected due to the consideration of generality performance validation for the EIMI technique. As well, for specimen 2, the impact locations of A, B, and C were selected to, respectively, verify anti-sensitivity capability, anti-inhomogeneous capability, and generality capability of the EIMI technique due to the composite structure with varying structural properties. The chosen impact locations on specimens 1 and 2 are all illustrated in Figures 18 and 19, separately. As for specimen 2, the impact position A is located at the vertical top of a specific sensor; the impact position B is located at an arbitrary point in the stiffened region; and the impact position C is located at an arbitrary point in the right bay region.

With the calculated IRF matrix networks, the reconstruction results match well with the actual force signals recorded in terms of maximum amplitude, force duration, and impulse. Furthermore, in order to assess the accuracies of the reconstructed forces, the relative average errors e_a corresponding to the above three parameters are needed for comparison, where the relative average error is defined as

$$e_a = \frac{1}{n}\sum_{i=1}^{n}\frac{calculated\ value - actual\ value}{actual\ value}\times 100\% \quad n = 1, 2, \ldots \tag{29}$$

To indicate the efficacy of the EIMI technique representatively, the evaluation results for unknown impacts of FR1 and FR2 on specimen 1 are only presented in Table 1. Meanwhile, in view of all of cases considered, for force reconstructions using the IRF matrix networks obtained from the training response data of the finite element method (FEM) simulations, the corresponding average error of maximum amplitude is 6%, the corresponding average error of force duration is 10.6%, and the corresponding average error of impulse is 10.1%; and for force reconstructions using the IRF matrix networks obtained from the training output data of the sensor measurements, the corresponding average error of maximum amplitude is 8%, the corresponding average error of force duration is 12.8%, and the corresponding average error of impulse is 11.3%.

Through the error evaluations and comparisons to the two approaches, it is easy to see that the force reconstructions using the training data from the FEM simulation can obtain better results than the reconstructions using the training data from the experimental measurements. However, this leads to the situation of different errors discovered in all the impact cases, mainly caused by several disturbed and unstable factors that may be known or unknown, for instance, from the constitutive property of CFRP material structure, there are (1) the deviations of material property of a carbon fiber prepreg lamina from the technical data sheets and manufacturing process and (2) the inconsistency of the structural property (e.g. stiffness) of a CFRP structure between the FEM calculation and actual CFRP product because of possible defects inside the real structure; from in situ impact experimental tests, there are also (1) accuracy of beating the training network nodes and (2) unpredictable impact conditions acting on the structures and so on.

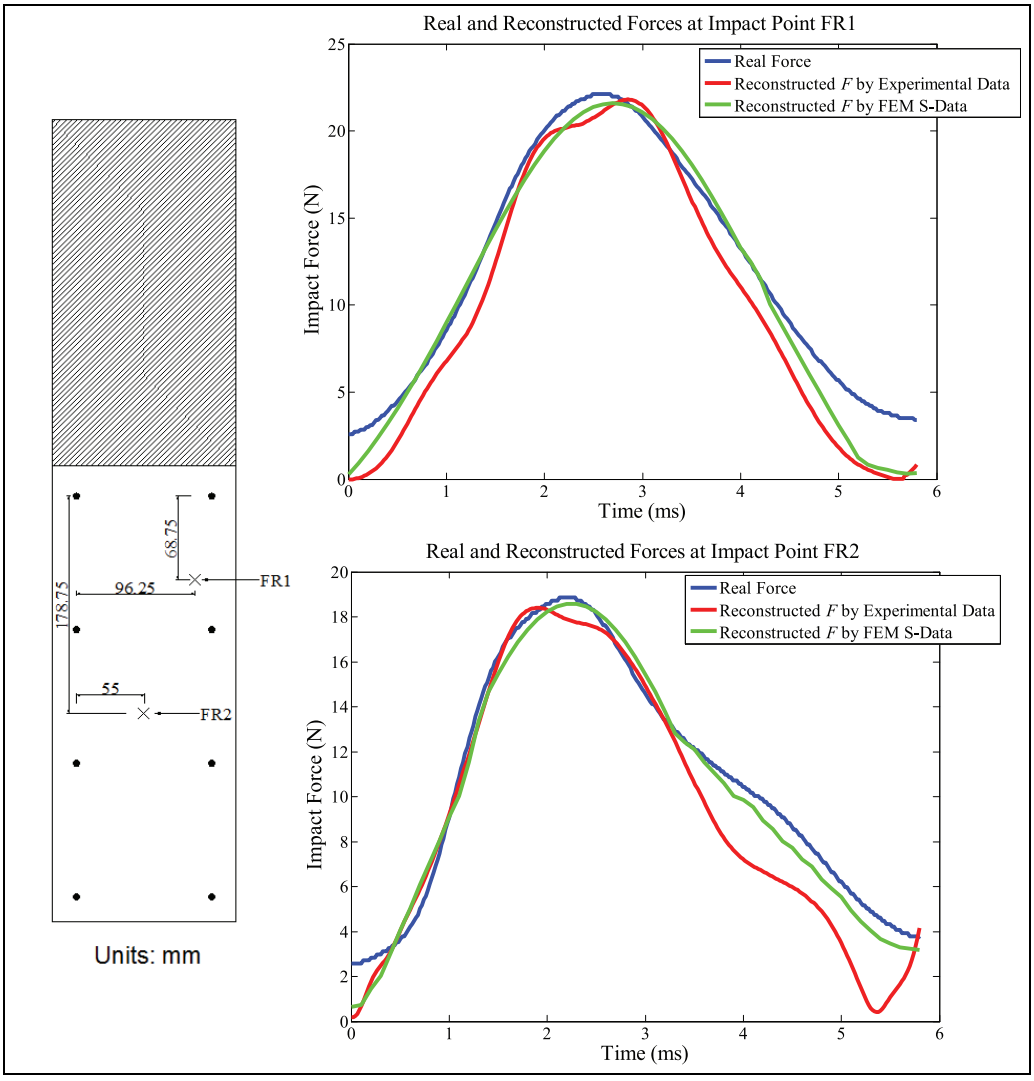

Figure 18. Force reconstructions on the cantilevered composite structure.

Table 1. Evaluation results for two unknown impact events of FR1 and FR2.

Impact events		Real	Estimation by experimental data	Estimation by FEM data
FR1	Maximum amplitude (unit: N)	22.1083	21.7480	21.6968
	Impulse (unit: N·s)	0.0704	0.0629	0.0658
FR2	Maximum amplitude (unit: N)	18.8395	18.3649	18.6815
	Impulse (unit: N·s)	0.0616	0.0543	0.0582

FEM: finite element method.

Impact identifications under random vibration effects

To verify the performance of the EIMI technique against vibration noise effects, unpredictable random vibration disturbance conditions were added to impact experimental tests. Then, through identification processing using the EIMI technique, the different results of force reconstructions are compared as shown in Figure 20, where they indicate that the impact forces are reconstructed under de-noising, within vibration noises of signal-to-noise ratio (SNR) of 20 and within vibration noises of SNR of 10. Finally, the average errors of force reconstructions

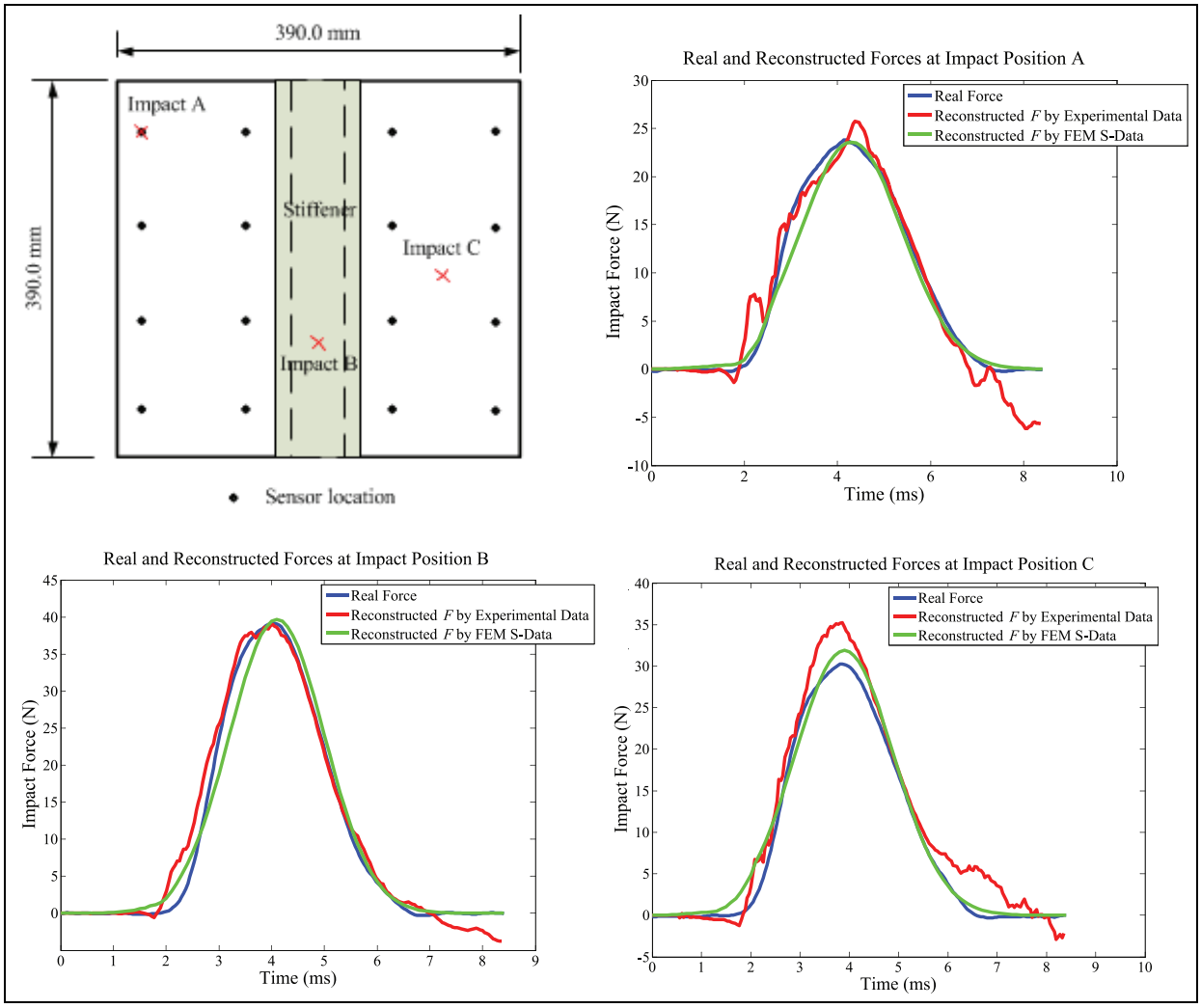

Figure 19. Force reconstructions on the stiffened composite structure.

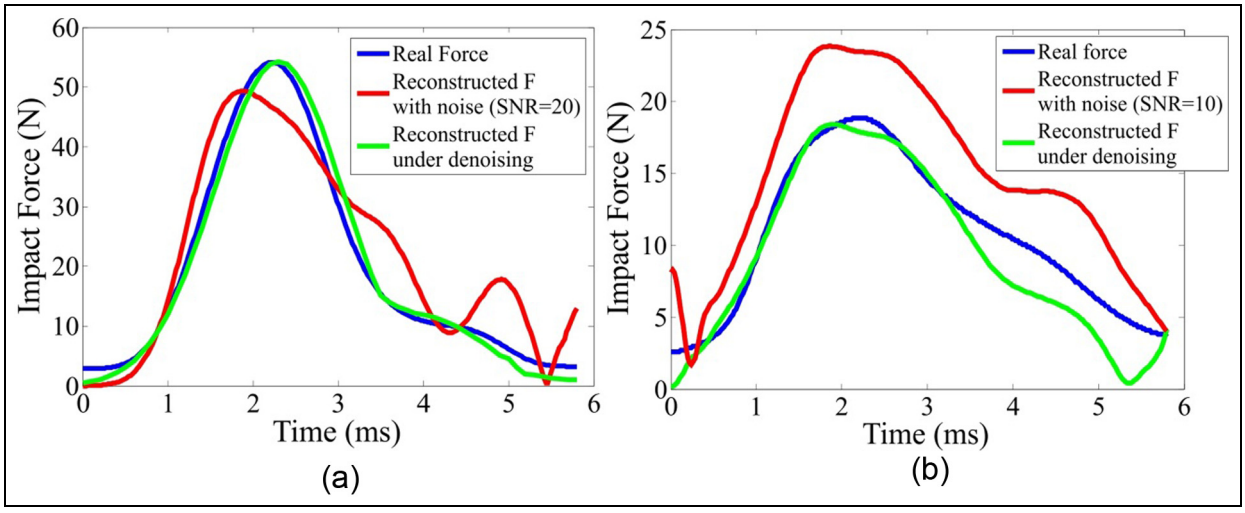

Figure 20. Comparison of impact identifications with noise contamination and under de-noising: (a) impact identification without and with noises of SNR = 20 and (b) impact identification without and with noises of SNR = 10.

Table 2. Impact evaluation results within vibration noises of SNR = 10 and 20.

Impact events		Real	Estimations by de-noising	Estimations within noises
SNR10	Maximum amplitude (unit: N)	18.84	18.38	23.83
	Impulse (unit: N·s)	0.0616	0.0543	0.0893
SNR20	Maximum amplitude (unit: N)	54.12	54.26	49.35
	Impulse (unit: N·s)	0.1130	0.1216	0.1398

SNR: signal-to-noise ratio.

within various noise contaminations are calculated out, which are both a little more than the results of de-noising implementations. The different results of impact identifications are indicated in Table 2. In general, in the condition of original output response signals with SNR = 20, the overall average error in force reconstruction is approximately 5% more than that of the de-noising implementation; in the condition of original output response signals with SNR = 10, the overall average error in force reconstruction is approximately 8.6% more than that of the de-noising implementation.

Discussion

However, it is worth noting that the requirement for the high accuracy of impact identification relies on the determination of the network of impulse response functions. However, to construct the appropriate network of IRFs for a given structure, it is concluded from two essential prerequisites:

1. More training data sets are indispensable in order to build a finer network of IRFs for a composite structure which has complex geometry and diverse mechanical properties within the whole structure. Therefore, to achieve this demand easily, the EIMI technique based on FE calculation models can be computationally fast to obtain any grid network from a practical requirement.
2. In view of the applicability of actual engineering, the transient dynamic responses due to impacts are duplicable at the symmetrical locations within a symmetric structure. But this may result in a challenge for large-scale structures if the location of each sensor was individual due to the practical demand. The response data from sensors may still need to be collected even if similar regions are at symmetrical locations in a complex structure. Nevertheless, the FE model-based EIMI technique can be flexible and fast to obtain the database from structural responses and overcome completely the above shortcoming, but also it can obtain any required response data set easily from any complex structure. Consequently, it could be qualified for applying the EIMI technique to monitor in real time any accidental impact event that causes possible damage in a large-scale aerospace composite structure.

Conclusion

This article presents a systematic impact monitoring and identification scheme. With the use of the smart distributed sensor networks defined, a novel real-time EIMI technique is developed to estimate the impact locations and force histories, including the information of the force magnitudes. In the entire automatic identification procedure, a precise forward model for a given structure can be established rapidly using the function module of the forward model generator. Meanwhile, by incorporating the dynamic state-space model, the impact forces can be reconstructed with a small number of IR functions from the optimal system parameters (a_i, b_j), calculated using the proposed FGAE during structure system modeling, which eliminates the need of numerous impact training tests for constructing the network of IR functions that cover a whole structure. Nevertheless, in impact positioning procedure, the initial impact locations can be estimated using the developed smoothed energy distribution method; afterward, on the basis of the results from the initial location estimations, each impacted region made up of four sensors can be determined. Subsequently, the accurate location coordinates of each impact can be updated further using the TOF-based quadrilateral sensor network positioning method proposed. This in situ real-time EIMI technique shows satisfactory success in predicting impact locations and estimating force histories for various composite structure configurations and under unpredictable vibration environments and thus verified its capability of impact monitoring and identification in complex adverse conditions. All the cases indicate that the EIMI technique is a good basis and potential tool for online onboard rapid diagnosis for impact monitoring of large-scale aerospace composite structures.

Declaration of Conflicting Interests

The author(s) declared no potential conflicts of interest with respect to the research, authorship, and/or publication of this article.

Funding

The author(s) disclosed receipt of the following financial support for the research, authorship, and/or publication of this article: The authors would like to gratefully acknowledge Lehrstuhl für Leichtbau for supporting this study.

References

1. Meo M, Zumpano G, Piggott M, et al. Impact identification on a sandwich plate from wave propagation responses. *Compos Struct* 2005; 71: 302–306.
2. Giurgiutiu V. *Structural health monitoring: with piezoelectric wafer active sensors*. Burlington, MA: Academic Press, 2007.
3. Qiu L, Yuan S, Liu P, et al. Design of an all-digital impact monitoring system for large-scale composite structures. *IEEE T Instrum Meas* 2013; 62: 1990–2002.
4. De Marchi L, Marzani A, Speciale N, et al. A passive monitoring technique based on dispersion compensation to locate impacts in plate-like structures. *Smart Mater Struct* 2011; 20: 035021.
5. Niri ED and Salamone S. A probabilistic framework for acoustic emission source localization in plate-like structures. *Smart Mater Struct* 2012; 21: 035009.
6. Ciampa F, Meo M and Barbieri E. Impact localization in composite structures of arbitrary cross section. *Struct Health Monit* 2012; 11: 643–655.
7. LeClerc J, Worden K, Staszewski W, et al. Impact detection in an aircraft composite panel—a neural-network approach. *J Sound Vib* 2007; 299: 672–682.
8. Ghajari M, Sharif-Khodaei Z, Aliabadi M, et al. Identification of impact force for smart composite stiffened panels. *Smart Mater Struct* 2013; 22: 085014.
9. Mallardo V, Aliabadi M and Khodaei ZS. Optimal sensor positioning for impact localization in smart composite panels. *J Intel Mat Syst Str* 2012; 24: 559–573.
10. Ribay G, Catheline S, Clorennec D, et al. Acoustic impact localization in plates: properties and stability to temperature variation. *IEEE Trans Ultrason Ferroelectr Freq Control* 2007; 54: 378–385.
11. Chen C, Li Y and Yuan F-G. Impact source identification in finite isotropic plates using a time-reversal method: experimental study. *Smart Mater Struct* 2012; 21: 105025.
12. Ciampa F and Meo M. Impact detection in anisotropic materials using a time reversal approach. *Struct Health Monit* 2012; 11: 43–49.
13. Park B, Sohn H, Olson SE, et al. Impact localization in complex structures using laser-based time reversal. *Struct Health Monit* 2012; 11: 577–588.
14. Seydel R and Chang F-K. Impact identification of stiffened composite panels: I. System development. *Smart Mater Struct* 2001; 10: 354–369.
15. Seydel R and Chang F-K. Impact identification of stiffened composite panels: II. Implementation studies. *Smart Mater Struct* 2001; 10: 370–379.
16. Peelamedu SM, Ciocanel C and Naganathan NG. Impact detection for smart automotive damage mitigation systems. *Smart Mater Struct* 2004; 13: 990.
17. Sharif-Khodaei Z, Ghajari M and Aliabadi M. Determination of impact location on composite stiffened panels. *Smart Mater Struct* 2012; 21: 105026.
18. Hiche C, Coelho CK and Chattopadhyay A. A strain amplitude-based algorithm for impact localization on composite laminates. *J Intel Mat Syst Str* 2011; 22: 2061–2067.
19. Park CY and Kim I-G. Prediction of impact forces on an aircraft composite wing. *J Intel Mat Syst Str* 2008; 19: 319–324.
20. Ahmari S and Yang M. Impact location and load identification through inverse analysis with bounded uncertain measurements. *Smart Mater Struct* 2013; 22: 085024.
21. Huang NE and Shen SS. *Hilbert-Huang transform and its applications*. Singapore: World Scientific, 2005.
22. Donoho DL. De-noising by soft-thresholding. *IEEE T Inform Theory* 1995; 41: 613–627.
23. Donoho DL and Johnstone JM. Ideal spatial adaptation by wavelet shrinkage. *Biometrika* 1994; 81: 425–455.
24. Brogan WL. *Modern control theory*. New Delhi, India; Chennai, India: Pearson Education, 1974.
25. Lennart L. *System identification: theory for the user*. Upper Saddle River, NJ: Prentice Hall PTR, 1999.
26. Goldberg D. *Genetic algorithms in search, optimization, and machine learning*. Reading, MA: Addison-Wesley, 1990.
27. Si L and Baier H. An advanced ensemble impact monitoring and identification technique for aerospace composite cantilever structures. In: *7th European workshop on structural health monitoring (EWSHM)*, Nantes, 8–11 July 2014.
28. *SAS/STAT® 92 user's guide: the LOESS procedure* (Book excerpt). Cary, NC: SAS Institute, Inc., 2008.